



ChemComm

New Semi-ladder Polymers for Ambipolar Organic Light-Emitting Transistors

Journal:	<i>ChemComm</i>
Manuscript ID	CC-FEA-07-2022-004087.R1
Article Type:	Feature Article

SCHOLARONE™
Manuscripts

New Semi-ladder Polymers for Ambipolar Organic Light-Emitting Transistors

Yachu Du, Dafei Yuan#, Mohammad A. Awais and Luping Yu*

Department of Chemistry and James Franck Institute, The University of Chicago, 929 E 57th Street,
Chicago, Illinois 60637, United States

#Materials Department, University of California, Santa Barbara, Engr II, UCSB Engineering II, Santa
Barbara, California, 93117, United States

Abstract: Organic light-emitting transistors (OLETs) combine the light-emitting and gate-modulated electrical switching functions in a single device. Over the past two decades, progress has been made in developing new fluorescent semiconductors and device engineering to improve the properties of OLETs. In this paper, we make a brief review of the achievement and disadvantages for the present polymer based OLETs, while highlight the recent development in semi-ladder polymers from our lab for new electroluminescent materials. The special folded molecular structures and unique aggregation states make these polymers suitable for exploration as OLET materials. A short conclusion is provided with a discussion on the challenges and future perspectives in this field.

Organic semiconducting polymers (OSCs) exhibit broad range of functions that resemble to inorganic semiconductors, yet unique features that distinguish them from inorganic counterparts. Functions such as semi-conductivity, electro-optical properties have been abundantly demonstrated and explored for various device applications, such as organic solar cells, organic field-effect transistors (OFETs) and organic light-emitting diodes (OLEDs), to name a few. They have attracted intense interests in the scientific and commercial communities for their pronounced and unique advantages including simple device structure,¹ low-cost solution processing,² capability to be fabricated into flexible and semitransparent devices,³ which conventional inorganic semiconductors could hardly achieve. Displays and smart digital gadgets, in human-machine interfaces, electronic artificial skin and wearable electronics are being developed based on organic solar cells, OFETs and OLEDs.⁴ These developments benefited from research progress in two fronts: new material synthesis and deeper understanding in underlining physical principles. A successful story is the development of OLEDs. Driven by the huge commercial benefit, the OLED materials were uprising to the center of the stage in display industry. On the other hand, the overall status of OFETs is not as glaring as the OLEDs in the current market. The innovation on the leading edge devices based on OFETs inspired further development in both material design and new device engineering.⁵

Because the scope of organic semi-conducting polymer is rather broad, this highlight is only focused on an important area, polymers for organic light emitting field effect transistor (OLET). OLET combines the features of electrical switching from field-effect transistors (FET) and light emitting property of OLED. These devices exhibit potential to simplify the fabrication of existing display systems and provide new option in areas, such as photonic communications and electrically pumped organic lasers.⁶ In an OLED device, electrons and holes are injected into a thin layer of emissive material with a thickness around hundred nanometers, sandwiched between the two electrodes. The electrons and holes in OLET devices are injected through the source-drain electrodes and recombine in the transport channel that is 10–100 μm long. This difference made the development of OLET more challenging than that of OLED because the transport channel is too long and mobility in organic OSC is too small and unbalanced between hole and electrons, which may lead to exciton quenching due to accumulated charges, significantly diminish the light emission efficiency.

An ideal light-emitting semiconductor for OLET requires appropriate energy levels to minimize charge injection barriers from metal contacts, ambipolar charge carrier mobility to ensure light emission at the center of the channel, proper band gap for color control and high

photoluminescent quantum yield (PLQY). All these parameters are hard to satisfy simultaneously in a single material and are often mutually exclusive. For example, materials demonstrating high charge carrier mobility usually exhibit efficient π - π stacking, and good electronic coupling to ensure efficient intermolecular charge transport. Unfortunately, efficient π - π stacking causes fluorescence quenching likely due to formation of exciplexes/excimers, charge transfer states and other non-radiative decay processes. In contrast, OLED materials show high quantum yield in solid state, but exhibit low charge carriers' mobility.⁷ Thus, mobility-fluorescence trade-off is one of the major barriers limiting material design for highly efficient OLETs.⁸ Several approaches to overcoming this trade-off have been reported in the literature, such as insertion of single-crystal active layers in single layer devices and multilayered device architectures, where charge transport and light-emitting functions are separated in different layers. In this highlight, we briefly discuss these approaches and focus on our recent effort on developing new materials to tackle this problem.

1. Brief review of the development of OLET polymers.

In 2003, Hepp and co-workers used the bottom gate bottom contact (BG-BC) structure to fabricate single-layer OFET devices with an organic small molecule semiconductor, tetracene.¹⁰ The OFET devices showed unipolar p-type behavior. During the evaluation of a transistor device, they observed light emission originating near the drain electrode. The FET

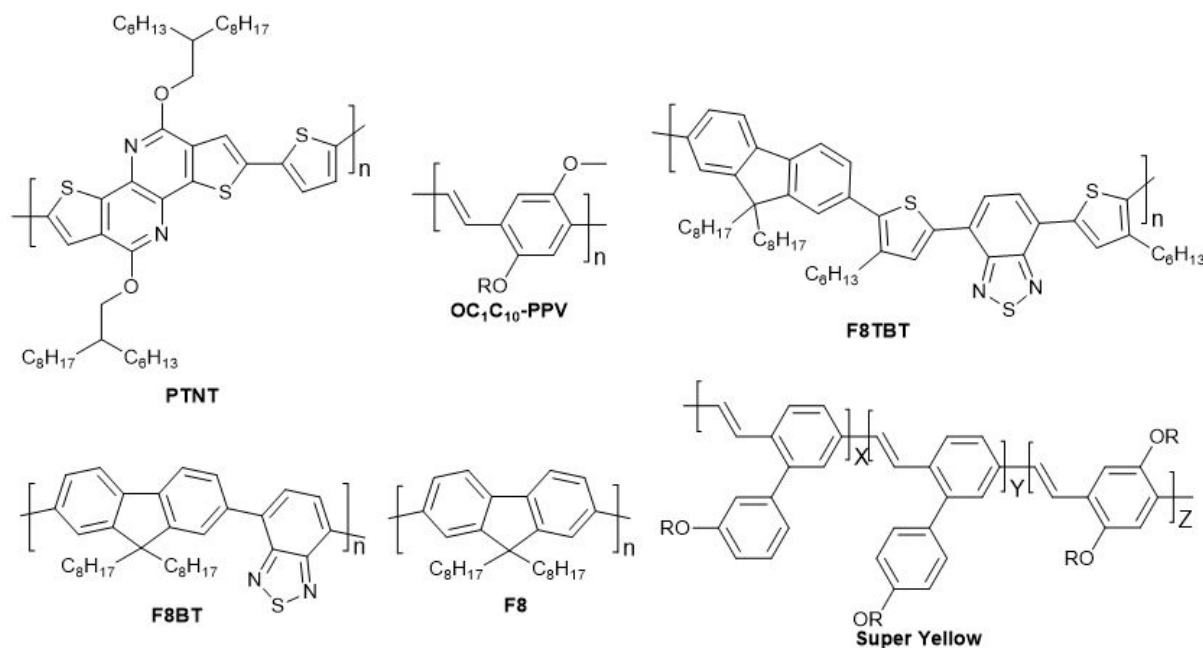


Figure 1. Chemical structures of the polymers in Table 1.

devices showed unipolar *p*-type behavior with the hole mobility of $5 \times 10^{-2} \text{ cm}^2 \text{ V}^{-1} \text{ s}^{-1}$ and a low EQE of $6.7 \times 10^{-5} \%$ due to the quenching at the metal drain electrode. This early result triggered increasing attentions on this novel organic electronic device.¹⁰⁻¹¹ Many small molecules like DPA and dNaAnt were employed in OLET fabrication with improved results.¹² The development of OLETs by using the small-molecule TBPMCN has recently achieved a remarkable EQE up to 10.5% at a brightness of 1000 cd m^{-2} by carefully selecting the hole blocking layer.¹³ However, these small molecules exhibit poor solubilities in common organic solvents, which renders the difficulty in device preparation. Some of the OLET devices had to utilize single crystals of these small molecules as the emitting layer. Polymeric materials are compatible with solution processing techniques for large scale manufacturing, and more promising candidates for OLET materials.

Unfortunately, the EL properties of polymer OLETs were lagging behind the small-molecule OLETs despite the advantage of solution processing.¹⁴ Several significant examples (Figure 1) are summarized in Table 1 for an overview of the polymer based OLETs' properties at current stage.

Similar to the unipolar small molecule materials, unipolar semiconducting polymers were also used to prepare OLET devices. Ahmad and coworkers chose a high electron mobility ($0.1 \text{ cm}^2 \text{ V}^{-1} \text{ s}^{-1}$) unipolar polymer to build OLET devices.¹⁵ The PLQY of PTNT in *o*-dichlorobenzene solution was found to be 45%. But the PLQY in neat films was reduced to 19%, which was attributed to strong π -stack induced molecular interactions. The OLETs exhibited mediocre electrical and optical characteristics with an EQE of 0.25% at 250 cd m^{-2} . The devices had spatially stable total emission areas which could not cover the whole channels independent from the gate voltage. This is a nuisance for the unipolar semiconducting polymers, limited their application as OLET materials.

Ambipolar semiconducting polymers exhibiting balanced hole and electron mobilities are more desirable to achieving better emitting characters. Zaumseil and coworkers fabricated the TC-BG single layer OLET by using OC₁C₁₀-PPV, which achieved a low PLQY value (10%) and an EQE up to 0.35% in 2006.¹⁶ The device was found ambipolar with electron and hole mobilities of 3×10^{-3} and $6 \times 10^{-4} \text{ cm}^2 \text{ V}^{-1} \text{ s}^{-1}$, respectively. A promising feature is that the position of the recombination and emission zone could be controlled by varying the applied gate voltages. It proved that electron and hole accumulation layers coexist for suitable bias condition. Later, they discovered that polymer F8BT exhibited a better balanced charge transport and high PLQY (55%), which contributed to the higher OLET EQE value (0.8%).¹⁷ Another related

polymer F8TBT exhibited more unbalanced charge transport and slightly lower PLQY (34%) compared to F8BT. The resulting OLET devices achieved the highest EQE of only 0.3%, which indicated the importance of the balance carrier mobility.

Further improvement in the properties of the OLET devices are possible via optimization on device structure. Gwinner and coworkers utilized F8BT as emission layer with different thickness of poly(methyl methacrylate) (PMMA) as gate dielectric (460-620 nm).¹⁸ The 460 nm of PMMA gave the device the highest EQE with a maximum value of 8.2%. However, the on/off ratio of these devices were far from satisfying (<10), which requires further optimization for pixel display applications.

In 2015, Kajii and coworkers utilized poly(9,9-dioctylfluorene) (F8) and F8BT to fabricate a bilayered OLET device.¹⁹ The F8 was spin-coated on top of F8BT as an electron blocking layer, also as good emission layer (PLQY=45%). The F8-F8BT bilayered device exhibited balance carrier mobility ($1.0 \times 10^{-3} \text{ cm}^2 \text{ V}^{-1} \text{ s}^{-1}$ for both), but the EQE value (0.6%) was not ideal.

Tri-layered structure is another common strategy to boost the properties of OLET devices, in which the emission layer is sandwiched by an n-type semiconducting layer and a p-type semiconducting layer to enhance the commonly poor carrier mobilities of these polymers. For example, Ullah and coworkers prepared OLET devices based on super yellow, a commercially available light emitting polymer, via this method. The emissive material with drain electrode was sandwiched between hole transport layer poly(2,5-bis(3-tetradecylthiophen-2-yl)thieno[3,2-b]thiophene) and electron transport layer Polyera Active-Ink N0700.²⁰ The resulting trilayered OLETs exhibited 2000 times higher EQEs (1.9%) and brightness (2100 cd m^{-2}) than single layer super yellow devices. The major drawback of this strategy is the device fabrication process. Each layer must be soluble in orthogonal solvents to avoid re-dissolution in the solution-casting procedure.

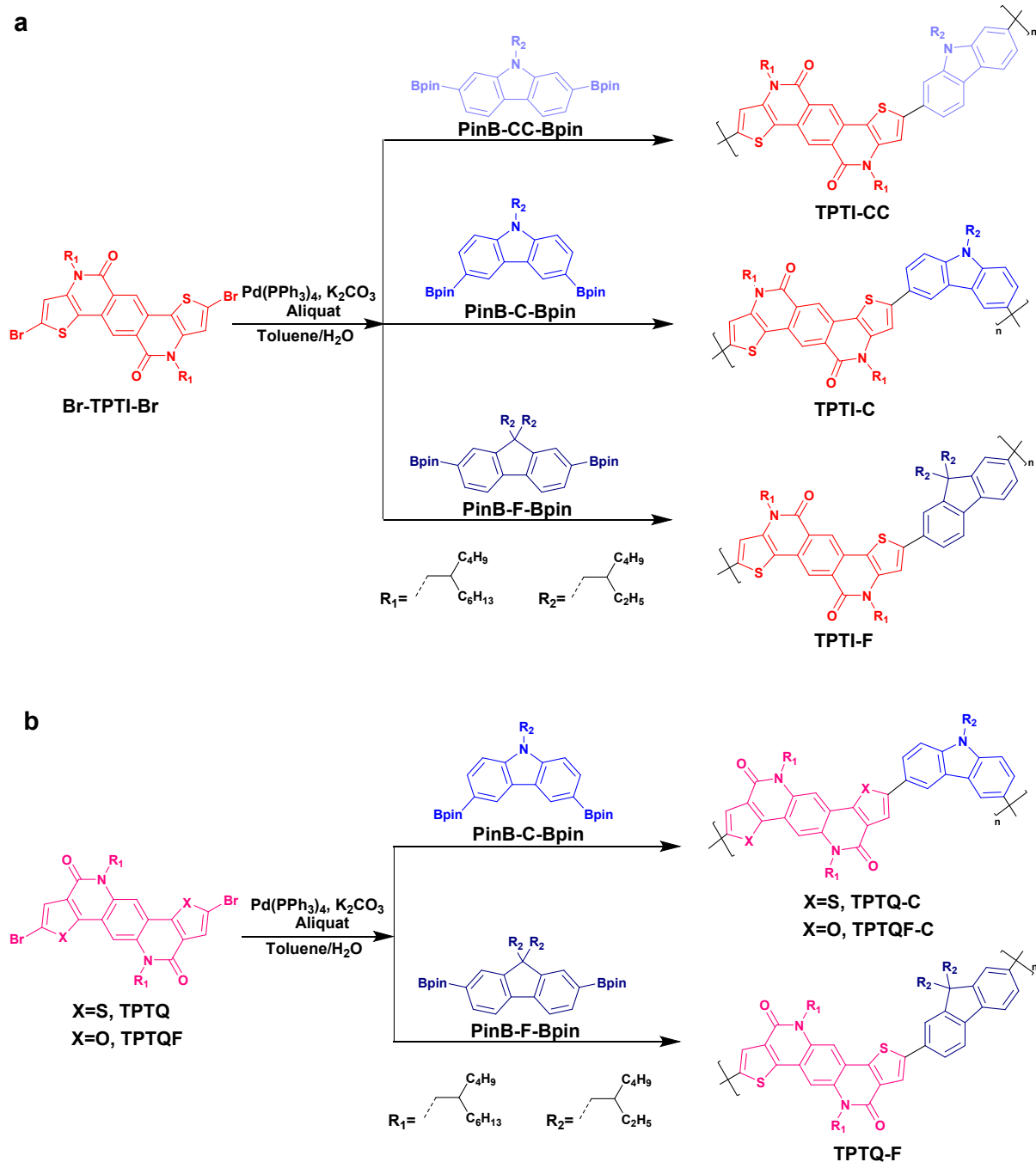
The discussion above showed that functional polymers bring the ease in processing, but accompanied with higher degree of energetic and conformational disorder than the small molecules. The emission characteristics in polymeric OLET are greatly influenced in solution and solid states.²¹ Moreover, the two contradictory requirements for OLET, high charge carrier mobility and high PLQY, are usually hard to satisfy in normal conjugated polymers. Thus, how to balance between the mobility and fluorescence trade-off is a dilemma that remains a great challenge to tackle in a single polymer system.⁸

Table 1. Carrier mobilities and optoelectronic properties of polymers discussed in this paper.

Polymer Name	Emission Wavelength (nm)	Hole Mobility ($\text{cm}^2 \text{V}^{-1} \text{s}^{-1}$)	Electron Mobility ($\text{cm}^2 \text{V}^{-1} \text{s}^{-1}$)	PLQY	Peak EQE
PTNT	570	-	1.0×10^{-1}	45%	0.25% ¹⁵
OC ₁ C ₁₀ -PPV	660	6.0×10^{-4}	3.0×10^{-3}	10%	0.35% ¹⁶
F8TBT	670	3.0×10^{-5}	6.0×10^{-4}	34%	0.4% ¹⁷
F8BT	575	7.5×10^{-4}	8.4×10^{-4}	54%	8.2% ¹⁸
F8 & F8BT	520/545	1.0×10^{-3}	1.0×10^{-3}	45% & 54%	0.6% ¹⁹
Super Yellow	550	1.2×10^{-1}	3.0×10^{-3}	60%	1.9% ²⁰

2. Semi-ladder polymers.

We recently developed luminescent semi-ladder co-polymers as OLET materials based on a weak donor-weak acceptor strategy. The results point to a possible solution to the dilemma



Scheme 1. Monomer structures and synthesis of semi-ladder polymers TPTI-CC, TPTI-C, TPTI-F, TPTQ-C, TPTQF-C and TPTQ-F.²⁷⁻²⁹

mentioned above. As shown in Scheme 1, the carbazole and fluorene derivatives are weak electron-donating units.²² Electron-deficient thieno[2',3':5,6]pyrido[3,4-g]thieno[3,2-c]-isoquinoline-5,11(4H,10H)-dione (TPTI), 5,11-bis(2-butyloctyl)-dihydrothieno[2',3':4,5]pyrido[2,3-g]thieno[3,2-c] quinoline-4,10-dione (TPTQ) and TPTQF were selected as the ladder-type building block to provide planarity, rigidity and charge transport.²³ The electron deficient monomers were copolymerized with carbazole/fluorene monomers via the Suzuki coupling reaction as shown in Scheme 1. Total six polymers were synthesized from three types of rigid weak acceptors and three types of fluorescent weak donors. For TPTI series of polymers, the TPTI-C was a cross-conjugated polymer while TPTI-F and TPTI-CC were fully conjugated ones. For TPTQ(F) series of polymers, the TPTQ-C and TPTQF-C were cross-conjugated polymers while TPTQ-F was fully conjugated one. Comparing monomer TPTQ(F) to TPTI, TPTQ(F) were more planar and crystalline compounds. This key difference led to the diversity in backbone planarity, LUMO energy levels and crystallinity of the resulting semi-ladder polymers, which was indicated by DFT calculation.

Figure 2 presents the HOMO/LUMO and the molecular geometry obtained from the DFT calculations at B3LYP level of theory using 6-31G** basis set. The chemical properties of the six semi-ladder polymers were listed in Table 2 including HOMO/LUMO energy level, electronic band-gap, molecular weight and polymer dispersity index. The molecular geometry simulation clearly showed that TPTI-CC, TPTI-F and TPTQ-F exhibited linear polymer backbones. It can be noticed that TPTQ-F had a higher planarity and deeper LUMO energy levels than TPTI-CC and TPTI-F; TPTI-C, TPTQ-C and TPTQF-C displayed coiled molecular backbones due to angled interconnection from carbazole moiety.

Table 2. Chemical properties of the six semi-ladder polymers.²⁷⁻²⁹

Polymer	HOMO (eV)	LUMO (eV)	E _g (eV)	M _w	M _n	PDI	PLQY
TPTI-CC	-5.20 ^a -4.91 ^b	-3.20 ^a -2.17 ^b	2.00	32428	23471	1.38	23%
TPTI-F	-5.48 ^a -4.93 ^b	-3.15 ^a -2.25 ^b	2.33	11963	9421	1.27	59%
TPTQ-F	-5.76 ^a -5.21 ^b	-3.38 ^a -2.46 ^b	2.75	55172	36012	1.53	77%
TPTI-C	-5.11 ^a -4.77 ^b	-3.09 ^a -1.78 ^b	2.02	17797	14070	1.26	21%
TPTQ-C	-5.44 ^a -5.03 ^b	-3.19 ^a -2.41 ^b	2.25	91767	32823	2.80	30%
TPTQF-C	-5.42 ^a -4.90 ^b	-3.04 ^a -1.92 ^b	2.38	50863	28835	1.76	50%

^aCalculated from oxidation onset of CV spectra. ^bCalculated from DFT.

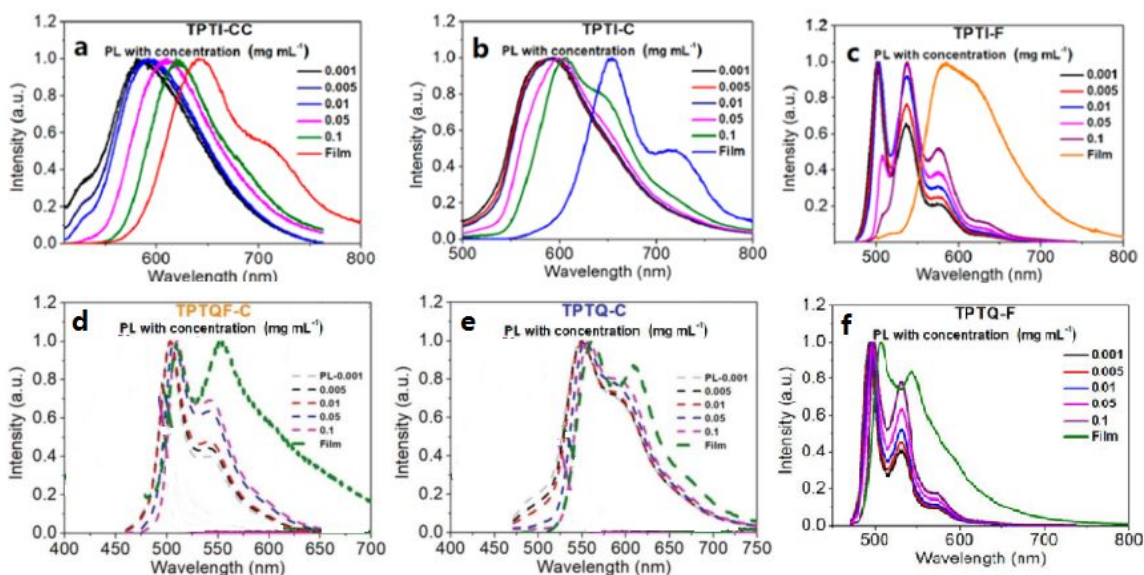


Figure 3. Photoluminescence (PL) spectra of (a)TPTI-CC, (b)TPTI-C, (c)TPTI-F, (d)TPTQF-C, (e)TPTQ-C and (f)TPTQ-F in chloroform solution and thin film.²⁷⁻²⁹

Fluorescence spectra showed the dominating 0-0 transition spectral characteristics from TPTI-CC and TPTQ-F, consistent with the formation of J-aggregates.²⁴ The emission spectra of TPTI-C, TPTI-F, TPTQ-C and TPTQF-C implied the formation of the H-aggregation.²⁵ In addition, normalized absorption spectra of TPTI-C, TPTQ-C and TPTQF-C showed almost no change in the spectral shape with decreasing concentration, indicating that H-aggregation exists even at the level of a single polymer chain, which is an evidence for polymer folding.^{26,27} The grazing-incidence wide-angle X-ray scattering gave us more information about the aggregation state. These polymers exhibited similar molecular packing ($d_{\pi-\pi}=3.6-4.1$ Å) but different crystallinities. TPTQ-F is the only strong crystalline polymer owing to its more

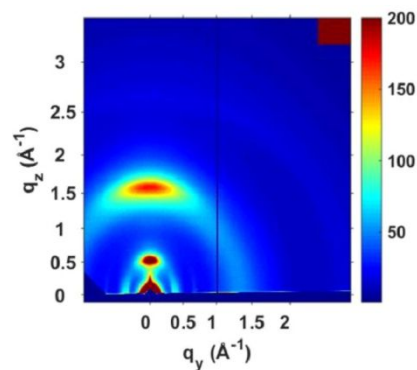


Figure 4. The grazing-incidence wide-angle X-ray scattering image of TPTQ-F. Reproduced from ref. 27 with permission from American Chemical Society, copyright 2021.

planar molecular backbone and interchain J-aggregations while other polymers were amorphous (Figure 4). Small angle X-ray scattering measurements in solution using advanced synchrotron light source used to analyze the structure of the coiled polymers.²⁶ The two polymers showed strong scattering intensity $I(q)$ at small scattering vector ($q < 0.3 \text{ \AA}^{-1}$), which corresponding to the calculated particle size of TPTQF-C (25.3 \AA) and that of TPTQ-C (24.3 \AA). The results is consistent with the simulated coiled structures (Figure 2).

The evaluation of PLQY of these polymers indicated that TPTQ-F and TPTI-F showed better performance due to excellent emitting character from fluorene monomer.²⁷ The semi-ladder polymers containing thiophenyl moiety exhibit limited photoluminescent quantum yield due to heavy atom effect (Table 2). A solution is to use furanyl moiety to replace thiophenyl one, leading to significant enhancement in PLQY.

Trilayered OLETs based on TPTI-CC, TPTI-C, TPTI-F, TPTQ-C and TPTQF-C

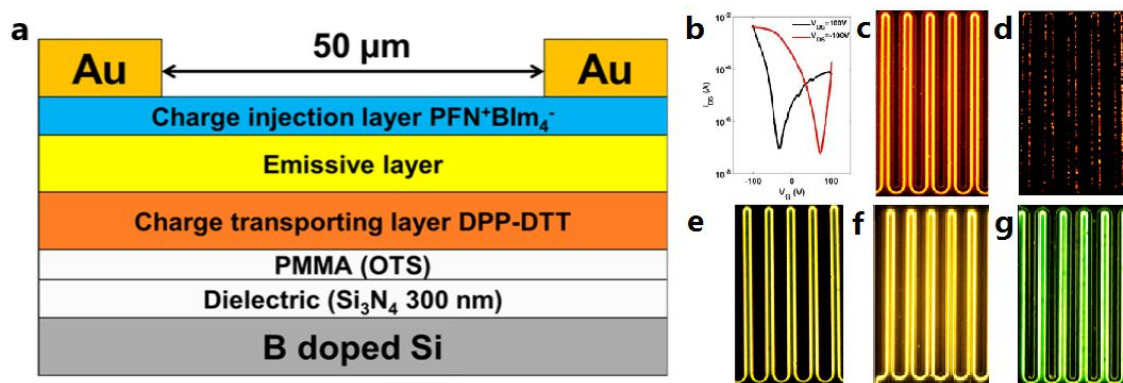


Figure 5. (a) Device configuration of OLET. (b) Transfer Curve of TPTQF-C. EL images of (c)TPTI-CC, (d)TPTI-C, (e)TPTI-F, (f)TPTQ-C and (g)TPTQF-C. Reproduced from ref. 28, 29 with permission from Royal Society of Chemistry, American Chemical Society, copyright 2020.

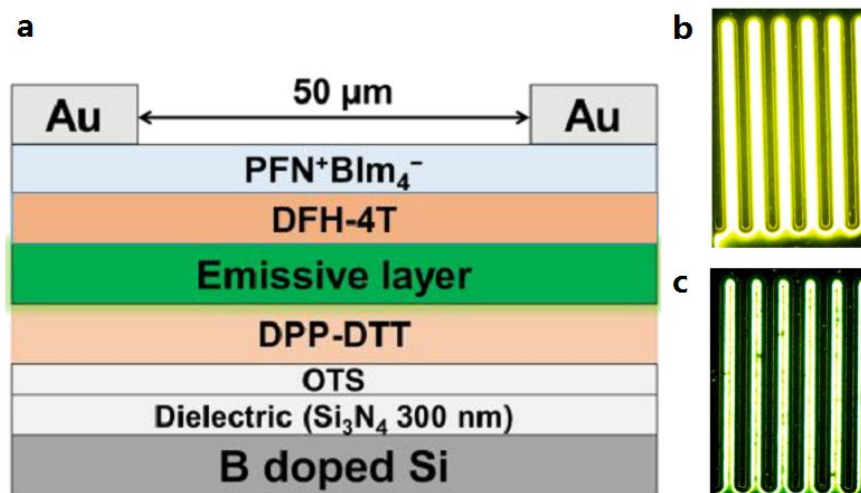


Figure 6. (a) Device configuration of OLET. EL images of (b)TPTQF-C and (c)TPTQ-F. Reproduced from ref. 27 with permission from American Chemical Society, copyright 2021. Reproduced from ref. 29 with permission from Royal Society of Chemistry, copyright 2020.

(Si₃N₄/PMMA(OTS)/DPP-DTT/emissive layer/ PFN⁺BIm₄⁻/Au) were fabricated (Figure 5a).²⁸ The OLET devices of these five polymers exhibited balanced ambipolar FET behavior with typical V-shape transfer curve (Figure 5b) and hole/electron mobility of 0.041/0.059, 0.39/0.23, 0.051/0.014, 0.025/0.032 and 0.35/0.51 cm² V⁻¹ s⁻¹, respectively. These OLET devices had good I_{on/off} ratio of 10⁵/10⁴, 10⁵/10⁴, 10⁵/10⁴, 10⁴/10⁴ and 10⁴/10³, respectively. Yellow/yellow-green emission were observed in the channels of the OLET devices (Figure 5c-g). Among these polymers, the devices fabricated with TPTQF-C displayed the best EL properties (EL intensity=216 nW, EQE_{max}=3.5%) because the coiled structure balanced the PLQY and charge transport.²⁹ It was also worth mentioning that this EQE value is comparable to the vacuum-deposited trilayered OLET device.²⁶

Further optimization of the device structure was feasible. Another electron transporting layer DFH-4T was inserted between the emissive layer and the charge injection layer. Moreover, DFH-4T showed high charge mobility of 0.5 cm² V⁻¹ s⁻¹ which was comparable with that of DPP-DTT. TPTQF-C and TPTQ-F were utilized in the new multilayered OLET devices (Figure 6a). As shown in Figure 6b, the much stronger yellow-green emission zone in these new TPTQF-

C devices extended significantly and nearly covered the whole channel.²⁹ This was in sharp contrast to the device shown in Figure 5g. This demonstrated that the injection charge carriers in the DFH-4T layer can transport efficiently and recombine with charge carriers from DPP-DTT bottom layer in the middle of the emissive layer. Higher EL intensity (2332 nW) and EQE (6.9%) was observed from the refined TPTQF-C OLETs. The OLETs with the same configuration were fabricated with TPTQ-F. The TPTQ-F exhibited high ambipolar charge mobilities and PLQY due to proper π - π interchain distance, which led to good performances in multilayered OLET devices. Yellow-green emission zone (Figure 6c) was broad and balanced in the channel under higher gate voltages ($V_{GS}=100$ V).²⁷ The ambipolar mobilities ($\mu_h=2.58\times 10^{-1}$ cm² V⁻¹ s⁻¹, $\mu_e=6.34\times 10^{-3}$ cm² V⁻¹ s⁻¹) were modest and not very balanced. Large $I_{on/off}$ ratios were obtained for both p-channel (10^5) and n-channel (10^4). The OLET devices performed the highest EL intensity of 414 nW and a max EQE of 5.3%, which was about two times higher than the less rigid and crystalline polymer TPTI-F (EL intensity=108 nW, EQE_{max}=2.8%).

These results revealed that the semi-ladder copolymers exhibiting a foldamer structure showed balanced electrical and light-emitting properties. The EQE and EL intensity achieved in OLET devices with TPTQF-C is the highest among the solution-processed multilayer OLET devices. It can be noted that there are two key points to design this type of semi-ladder polymers. Firstly, ring fusion introduces rigidity into the molecular system, decreasing the effective vibrational modes available for non-radiative decay and thus improving light emission which improves the PLQY. Secondly, the folded backbone introduces weak aggregation due to structural restraint and yet allow for effective overlap between chromophores for charge transport. These two key points ameliorate the PLQY/charge transfer dilemma mentioned above.

3. Conclusion and outlook.

In summary, this feature article highlights our recent work on semi-ladder polymers. These polymers were shown to exhibit significant PLQY, EQE and EL intensities in solvent-processed OLET devices. The electrical and EL properties are influenced by their molecular structures and aggregation states. There are three take-home lessons. 1) The rigid and electron deficient monomer can reduce the degree of energetic disordered of the semi-ladder polymers that contributed to better fluorescence and charge transport. 2) The foldamer structure can provide compromised solution to the dilemma between light emission and charge transport. 3) The inserted charge transporting layers that balanced charge injection and transport so that excitons are formed away from the edge of electrodes to avoid exciton quenching.

At the current stage, it's undeniable that many challenges exist in the development of

OLET devices. Other than the problems in molecular design we mentioned, there are more challenges to satisfy the actual application requirements, for example, pixelated luminescence control. Development of high-performance materials and new device structures is required to prepare high performance OLET devices.³⁰ Except small-molecule, single crystal and polymers, the researchers are also attempting organic heterojunctions^{26, 31}, molecular charge-transfer cocrystals³² and thermally activated delayed fluorescence emitters³³ as the emitting layer to improve the overall performance. Moreover, hybrid devices utilizing carbon nanotube, graphene and perovskite as the transporting layer may become an alternative way to further enhance the properties of OLET devices.³⁴ Last but not the least, the OLET device with new developed configuration, for instance vertical light-emitting transistor³⁵ and overlapping-gate OLET³⁶, are expected to make breakthroughs in the field of reducing working voltage and fabricate RGB color OLETs.

ACKNOWLEDGMENT

This work was supported by NSF (CHE-2102102).

References

1. Geffroy, B.; Le Roy, P.; Prat, C., *Polymer international* **2006**, *55* (6), 572-582.
2. Allard, S.; Forster, M.; Souharce, B.; Thiem, H.; Scherf, U., *Angewandte Chemie International Edition* **2008**, *47* (22), 4070-4098.
3. Traverse, C. J.; Pandey, R.; Barr, M. C.; Lunt, R. R., *Nature Energy* **2017**, *2* (11), 849-860.
4. Sokolov, A. N.; Tee, B. C.; Bettinger, C. J.; Tok, J. B.-H.; Bao, Z., *Accounts of chemical research* **2012**, *45* (3), 361-371.
5. Sirringhaus, H., *Advanced materials* **2014**, *26* (9), 1319-1335.
6. a. Zhang, C.; Chen, P.; Hu, W., *Small* **2016**, *12* (10), 1252-1294; b. Muccini, M.; Koopman, W.; Toffanin, S., *Laser & Photonics Reviews* **2012**, *6* (2), 258-275.
7. Nikolka, M.; Broch, K.; Armitage, J.; Hanifi, D.; Nowack, P. J.; Venkateshvaran, D.; Sadhanala, A.; Saska, J.; Mascal, M.; Jung, S.-H., *Nature communications* **2019**, *10* (1), 1-9.
8. aZhang, X.; Dong, H.; Hu, W., *Advanced Materials* **2018**, *30* (44), 1801048; bLiu, D.; Li, C.; Niu, S.; Li, Y.; Hu, M.; Li, Q.; Zhu, W.; Zhang, X.; Dong, H.; Hu, W., *Journal of Materials Chemistry C* **2019**, *7* (20), 5925-5930.
9. Yuan, D.; Sharapov, V.; Liu, X.; Yu, L., *ACS omega* **2019**, *5* (1), 68-74.
10. Hepp, A.; Heil, H.; Weise, W.; Ahles, M.; Schmechel, R.; von Seggern, H., *Physical review letters* **2003**, *91* (15), 157406.
11. Rost, C.; Karg, S.; Riess, W.; Loi, M. A.; Murgia, M.; Muccini, M., *Applied physics letters* **2004**, *85* (9), 1613-1615.
12. Qin, Z.; Gao, H.; Liu, J.; Zhou, K.; Li, J.; Dang, Y.; Huang, L.; Deng, H.; Zhang, X.; Dong, H., *Advanced Materials* **2019**, *31* (37), 1903175.
13. Hu, Y.; Song, L.; Zhang, S.; Lv, Y.; Lin, J.; Guo, X.; Liu, X., *Advanced Materials Interfaces* **2020**, *7* (17), 2000657.
14. aUllah, M.; Armin, A.; Tandy, K.; Yambem, S. D.; Burn, P. L.; Meredith, P.; Namdas, E. B., *Scientific Reports* **2015**, *5* (1), 1-6; bRoelofs, W. C.; Adriaans, W. H.; Janssen, R. A.; Kemerink, M.; de Leeuw, D. M., *Advanced Functional Materials* **2013**, *23* (33), 4133-4139.
15. Ahmad, V.; Shukla, A.; Sobus, J.; Sharma, A.; Gedefaw, D.; Andersson, G. G.; Andersson, M. R.; Lo, S. C.; Namdas, E. B., *Advanced Optical Materials* **2018**, *6* (21), 1800768.
16. Zaumseil, J.; Friend, R. H.; Sirringhaus, H., *Nature materials* **2006**, *5* (1), 69-74.

17. Zaumseil, J.; McNeill, C. R.; Bird, M.; Smith, D. L.; Paul Ruden, P.; Roberts, M.; McKiernan, M. J.; Friend, R. H.; Sirringhaus, H., *Journal of Applied Physics* **2008**, *103* (6), 064517.
18. Gwinner, M. C.; Kabra, D.; Roberts, M.; Brenner, T. J.; Wallikewitz, B. H.; McNeill, C. R.; Friend, R. H.; Sirringhaus, H., *Advanced Materials* **2012**, *24* (20), 2728-2734.
19. Kajii, H.; Tanaka, H.; Kusumoto, Y.; Ohtomo, T.; Ohmori, Y., *Organic Electronics* **2015**, *16*, 26-33.
20. Ullah, M.; Tandy, K.; Yambem, S. D.; Aljada, M.; Burn, P. L.; Meredith, P.; Namdas, E. B., *Advanced Materials* **2013**, *25* (43), 6213-6218.
21. Leventis, A.; Royackers, J.; Rapidis, A. G.; Goodeal, N.; Corpinot, M. K.; Frost, J. M.; Bučar, D.-K. i.; Blunt, M. O.; Cacialli, F.; Bronstein, H., *Journal of the American Chemical Society* **2018**, *140* (5), 1622-1626.
22. aZaumseil, J.; Donley, C. L.; Kim, J. S.; Friend, R. H.; Sirringhaus, H., *Advanced Materials* **2006**, *18* (20), 2708-2712; bTomkeviciene, A.; Grazulevicius, J. V.; Volyniuk, D.; Jankauskas, V.; Sini, G., *Physical Chemistry Chemical Physics* **2014**, *16* (27), 13932-13942.
23. Jung, I. H.; Lo, W.-Y.; Jang, J.; Chen, W.; Zhao, D.; Landry, E. S.; Lu, L.; Talapin, D. V.; Yu, L., *Chemistry of Materials* **2014**, *26* (11), 3450-3459.
24. Spano, F. C.; Silva, C., *Annual review of physical chemistry* **2014**, *65*, 477-500.
25. Birks, J.; Christophorou, L., *Spectrochimica Acta* **1963**, *19* (2), 401-410.
26. Capelli, R.; Toffanin, S.; Generali, G.; Usta, H.; Facchetti, A.; Muccini, M., *Nature materials* **2010**, *9* (6), 496-503.
27. Yuan, D.; Awais, M. A.; Sharapov, V.; Liu, X.; Neshchadin, A.; Chen, W.; Yu, L., *Journal of the American Chemical Society* **2021**, *143* (13), 5239-5246.
28. Yuan, D.; Awais, M. A.; Sharapov, V.; Liu, X.; Neshchadin, A.; Chen, W.; Yu, L., *Chemistry of Materials* **2020**, *32* (11), 4672-4680.
29. Yuan, D.; Awais, M. A.; Sharapov, V.; Liu, X.; Neshchadin, A.; Chen, W.; Bera, M.; Yu, L., *Chemical science* **2020**, *11* (41), 11315-11321.
30. Liu, Y.; Guo, Y.; Liu, Y., *Small Structures* **2021**, *2* (1), 2000083.
31. Song, L.; Hu, Y.; Zhang, N.; Li, Y.; Lin, J.; Liu, X., *ACS Applied Materials & Interfaces* **2016**, *8* (22), 14063-14070.
32. Zhu, W.; Zheng, R.; Zhen, Y.; Yu, Z.; Dong, H.; Fu, H.; Shi, Q.; Hu, W., *Journal of the American Chemical Society* **2015**, *137* (34), 11038-11046.
33. Song, L.; Hu, Y.; Liu, Z.; Lv, Y.; Guo, X.; Liu, X., *ACS Applied Materials & Interfaces* **2017**, *9* (3), 2711-2719.
34. Park, B.; Lee, W. S.; Na, S. Y.; Huh, J. N.; Bae, I.-G., *Scientific reports* **2019**, *9* (1), 1-11.

35. Hlaing, H.; Kim, C.-H.; Carta, F.; Nam, C.-Y.; Barton, R. A.; Petrone, N.; Hone, J.; Kymissis, I., *Nano Letters* **2015**, *15* (1), 69-74.
36. Lee, J. H.; Ke, T. H.; Genoe, J.; Heremans, P.; Rolin, C., *Advanced Electronic Materials* **2019**, *5* (1), 1800437.